A Physical Model of Potassium Channel Activation: From Energy Landscape to Gating Kinetics

Daniel Sigg and Francisco Bezanilla
Department of Physiology and Department of Anesthesiology, David Geffen School of Medicine, University of California at Los Angeles, Los Angeles, California 90095

ABSTRACT We have developed a method for rapidly computing gating currents from a multiparticle ion channel model. Our approach is appropriate for energy landscapes that can be characterized by a network of well-defined activation pathways with barriers. To illustrate, we represented the gating apparatus of a channel subunit by an interacting pair of charged gating particles. Each particle underwent spatial diffusion along a bistable potential of mean force, with electrostatic forces coupling the two trajectories. After a step in membrane potential, relaxation of the smaller barrier charge led to a time-dependent reduction in the activation barrier of the principal gate charge. The resulting gating current exhibited a rising phase similar to that measured in voltage-dependent ion channels. Reduction of the two-dimensional diffusion landscape to a circular Markov model with four states accurately preserved the time course of gating currents on the slow timescale. A composite system containing four subunits leading to a concerted opening transition was used to fit a series of gating currents from the *Shaker* potassium channel. We end with a critique of the model with regard to current views on potassium channel structure.

INTRODUCTION

The voltage sensitivity of ion channels stems from charge-field interactions that alter the conformational energy landscape of the protein. A change in the applied membrane potential (V) initiates the relaxation of charged regulatory domains within the channel protein, generating a gating current (i_g). On the physiologically relevant timescale of milliseconds to seconds, experimental findings of multiexponential decay (Stefani et al., 1994) and shot noise (Conti and Stühmer, 1989; Sigg et al., 1999) in the gating current imply that the energy pathway for channel activation possesses multiple barriers; in other words, the landscape is hilly. Given sufficiently rugged landscapes, a coarse-graining procedure may be applied to construct discrete-state Markov (DSM) models that preserve activation kinetics on the physiological timescale. The primary advantage of a DSM model is the straightforward computation of gating currents, although information about fast events is lost. Among various DSM models used to describe gating in the *Shaker*-like family of potassium channel, variations of the ZHA model (Zagotta et al., 1994) have recently received attention (Schoppa and Sigworth, 1998; Smith-Maxwell et al., 1998; Bao et al., 1999; Ledwell and Aldrich, 1999; Kanevsky and Aldrich, 1999; Mannuzzu and Isacoff, 2000; Tang et al., 2000). These models acknowledge the tetrameric symmetry of the *Shaker* channel by containing four parallel pathways of activation. Once all four subunits reach a permissive state, the pathways merge, whereupon the channel likely experiences an additional series of concerted transitions before opening (Schoppa and Sigworth, 1998; Ledwell and Aldrich, 1999).

Here, we sketch a minimal physical model of the potassium channel with ZHA-like features. In our model, the gating mechanism of a single channel subunit is made up of interacting charged particles that make transitions across hydrophobic regions of the protein. For the sake of simplicity we assigned a maximum of two metastable states for each gating particle. In doing so we addressed the interesting problem of how to generate a so-called rising phase in the gating current with a collection of two-state particles. The rising phase is a feature of the gating current observed in *Shaker* and other voltage-dependent channels, defined as an initial upward deflection of i_g preceding the main decay phase. The significance of the rising phase is unclear; it is generally observed by stepping from a negative holding potential to membrane potentials that are sufficiently positive to activate (open) the channel (Keynes and Elinder, 1998).

It is important to realize that it is impossible to generate a rising phase in i_g from an ensemble of independent two-state particles. The reason is that each particle in the ensemble relaxes with a positive charge movement in response to a positive change in V (this is true even for negatively charged particles). More specifically, a collection of N independent particles yields a gating current that is the sum of N positive amplitude exponents. Such an ensemble cannot produce a rising phase, which requires at least one negative amplitude component. On the other hand, a single particle with a minimum of two sequential transitions will generate a rising phase in i_g if the first transition is slower or displaces less gating charge than the second transition (Bezanilla and Taylor, 1982). Of course, such a particle violates our two-state requirement. However, and this is the basis of the model we propose here, a system composed of interacting two-state particles may generate a rising phase under favorable circumstances. The reason this is possible is that energy

Submitted September 13, 2002, and accepted for publication February 6, 2003.

Address reprint requests to Dr. Francisco Bezanilla, Dept. of Physiology, University of California at Los Angeles, 10833 Le Conte Ave., Los Angeles, CA 90095. Tel.: 310-825-2735; Fax: 310-794-9612; E-mail: fbezanil@ucla.edu.

0006-3495/03/06/3703/14 $2.00

interactions lead to an unequally weighted pair of two-transition activation pathways. Conditions may be chosen such that the more probable of the two pathways satisfies the conditions for a rising phase, leading, on average, to the desired form of i_g.

A cross-sectional view of a candidate model is shown in Fig. 1. It consists of two charged particles; each undergoes spatial diffusion governed by a potential of mean force. The particles move along the membrane perpendicular (parallel to electric field lines, which are assumed to be nondivergent). The relatively hydrophobic region within the channel is responsible for the barrier experienced by the charges as they traverse the membrane field. The gate particle has the larger positive valence and traverses a greater fraction of the membrane potential drop; thus it contributes the majority of the gating charge displacement. The role of the negatively charged barrier particle is to modulate the height of the gate particle's transition barrier through electrostatic interactions.

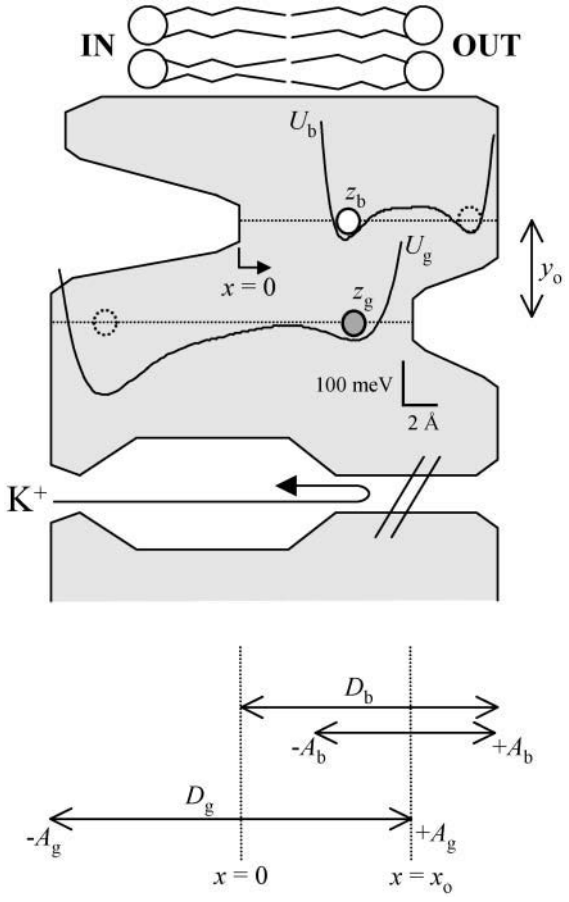

FIGURE 1 Single subunit model ($V = 0$ mV). The membrane potential V is defined as the intracellular (*IN*) potential with reference to the extracellular space (*OUT*). Outward gating currents are positive. Permeant ions such as K^+ are prevented from traversing the pore, abolishing the ionic current. The positively charged gate particle is depicted as a dark sphere (z_g) fluctuating along the lower dotted line. Its movement is governed by: the bistable energy profile, U_g; electrostatic interactions with a similarly fluctuating barrier molecule, z_b (in *white*); and thermal forces. Dotted circles represent vacant metastable states. The configuration depicted here (*C4*) is the most stable for $V = 0$ mV. The values of model parameters are listed in Table 1.

Applying a large negative resting potential drives the two particles to opposite sides of the membrane; this, despite an electrostatic attraction that tends to bring them together. After suddenly removing the membrane potential (voltage-clamp experiment), The system relaxes to a new equilibrium state in which the particles have crossed transition barriers and now reside in close proximity to each other (illustrated in Fig. 1). The gating current is a record of the relaxation process. We designed a model in which the barrier particle, the lesser of the two gating charges, is likely to transition first, thereby reducing the distance between the two particles, and significantly accelerating the ensuing transition of the gate particle. Ignoring for the moment the contribution of the barrier particle to the gating current (although it, too, contributes gating charge), the model renders the dominant contributor to i_g—the transition of the gate particle—non-Markovian; that is, the number of gate transitions per unit time in a population of channel subunits is a function of the barrier particle position, and increases with time of depolarization. The interplay with a fluctuating environment introduces memory into the transition rate of the gating particle, and a rising phase is made possible. The above scenario must be balanced by the alternative series of events—a gate particle transition followed by a barrier particle transition—that does not produce a rising phase but which can be made less probable through proper choice of parameters.

METHODS

Details of the two-particle subunit model

The free energy of the subunit model is given by the sum of two single-particle terms, an electrostatic interaction potential, and a voltage-dependent term:

$$W_{g,b}(w_g, x_b, V) = U_g(x_g) + U_b(x_b) + U_{g,b}(x_g, x_b) + U_v(x_g, x_b, V);$$

$$U_g = U_g^o\left[(-0.25)\left(\frac{x_g}{½A_g}\right)^4 + (0.08)\left(\frac{x_g}{½A_g}\right)^6\right], \quad \{-A_g \le x_g \le A_g\}$$

$$U_b = U_b^o\left[(-0.25)\left(\frac{x_b - x_o}{½A_b}\right)^4 + (0.08)\left(\frac{x_b - x_o}{½A_b}\right)^6\right], \quad \{x_o - A_b \le x_b \le x_o + A_b\}$$

$$U_{g,b} = \frac{1}{4\pi\varepsilon}\frac{z_g z_b}{r},$$

$$U_v = -q_{obs}(V - V_o) = -(q_g + q_b)\left(V - \frac{q_g V_g + q_b V_b}{q_g + q_b}\right). \quad (1)$$

The gating particles move in a straight line along the direction perpendicular to the membrane, with displacements: x_g (i.e., gate) and x_b (i.e., barrier). The distance between the two particles is $r = ((x_g - x_b)^2 + y_o^2)^{1/2}$, where y_o is the minimum separation. The observable gating charge displacement q_{obs} is the sum of the individual gating charges: $q_g = z_g(x_g + A_g)/D_g$, and $q_b = z_b(x_b - x_o - A_b)/D_b$, where A_i is the range and D_i is the effective membrane thickness for the particle i. V_g and V_b are the voltage offsets for the respective particles. The dielectric constant $K = \varepsilon/\varepsilon_o$, where ε_o is the permittivity of free space ($1/4\pi\varepsilon_o = 1.44 \times 10^4$ meV $\times$ Å/eu^2). The values of all model parameters are listed in Table 1. A contour map of $W_{g,b}$ is shown in Fig. 2 *A* for resting ($V = -120$ mV) and depolarizing ($V = 10$ mV) potentials.

Numerical analysis

Kinetic analysis of the subunit model fell into two categories. Monte Carlo simulation employed the full state space of the model and produced accurate results, but was exceedingly slow (i.e., overnight runs on a desktop PC to simulate one set of conditions). Reduction to a smaller state space dramatically increased the speed of computation, but the increased efficiency invariably came at a cost with respect to detail and accuracy, which we attempted to minimize.

The sufficiently large transition barriers and well-defined kinetic pathways evident in the two-dimensional energy landscape (Fig. 2 *A*) made it possible to consider a reduced four-state circular DSM model (Fig. 2 *B*), where the combinatorial set of stable particle configurations determines the group of states C1–C4. Kinetic pathways were characterized as potentials of mean force (PMF) along suitable reaction coordinates. The PMF, with respect to the gating charge q, is given by

$$W_q = -kT \ln\left(\int_{\{x\}} \exp\left(\frac{-W_{\{x\}}}{kT}\right) d\{x\}\right), \qquad (2)$$

where $\{x\}$ are the spatial variables x_g and x_b, and the integration is carried out over all pairs of $\{x\}$ consistent with the value of q and located within boundaries of interest. We employed the variables q_g, q_b, and q_{obs} as reaction coordinates, often integrating over a subset of $\{x\}$ to select specific pathways.

The kinetics of a one-dimensional reaction coordinate were assumed to be governed by the Smoluchowski equation, which, in electrical units, is given by

$$\frac{\delta}{\delta t}p = -\frac{\delta}{\delta q}\left[\frac{-W'(q)}{R(q)}p - \frac{kT}{R(q)}\frac{\delta}{\delta q}p\right], \qquad (3)$$

where $p(q,t)$ is the probability density of gating charge displacement, kT is the thermal energy, and the electrical resistance R is related to the spatial friction coefficient f by a factor of $(D/z)^2$. Each particle was assigned an individual value of resistance (R_b or R_g). The choice of R is in some sense arbitrary when considering barrier-hopping kinetics; an increase in the activation energy can be used to compensate for a decrease in the value of R, and vice versa. Thus, both particles might have shared the same value of R without significantly altering the slow kinetics of the model. However, the treatment of two resistance values in the reduction of Eq. 1 to a one-dimensional PMF landscape is of interest, as we shall demonstrate later. The use of Eq. 3 in computing gating currents from a one-dimensional landscape has been presented in detail by Sigg et al. (1999).

TABLE 1 Physical parameters

	Single subunit model		*Shaker* simulation	
Variable	Gate	Barrier	Gate	Barrier
z_i (eu)	3	−2	2.57 ± 0.03*	−1.85 ± 0.02*
f_i (meV × ms/Å^2)	1	0.2	0.01 ± 0.01*	0.26 ± 0.05*
R_i (mV × ms/eu)	0.44†	11.3†	0.60†	17.1†
D_i	20	15	20	15
A_i (Å)	10	5	10	5
U_i^o (meV)	400	350	363 ± 39*	264 ± 18*
V_i (mV)	110	30	114 ± 5*	28 ± 2*
K (dielectric const.)	30		26.9 ± 0.6*	
x_o (Å)	10		10	
y_o (Å)	5		5.21 ± 0.08*	

*Fitted variables (mean ± SD).
†Derived value.

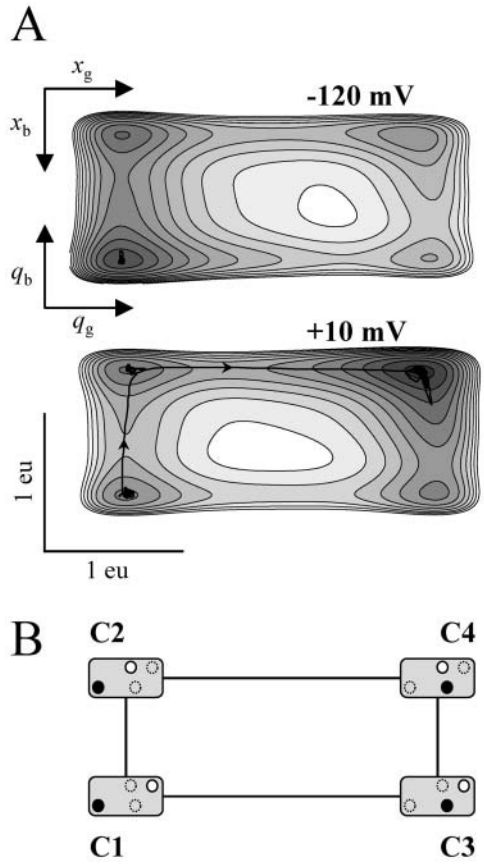

FIGURE 2 Energy landscape ($W_{g,b}$) of the single subunit model. (*A*) Contour map for two voltages with iso-potential lines 50 meV (2 kT) apart. A single Monte Carlo trajectory filtered at 20 kHz is superimposed onto the landscapes at rest (−120 mV) and during activation (+10 mV). Small arrows indicate the direction of activation. (*B*) Reduction to a DSM representation. States C1–C4 are evident as minima in the energy landscape. The relative positions of gating particles are shown schematically using the same half-tone scheme used in Fig. 1.

For adequately high barriers (>5 kT), transition rate constants reach the Markovian value rapidly and may be reliably obtained by taking the inverse of the mean first passage time (T_{mfp}) from initial state (q_o) on the reaction side of the barrier to a final absorbing state (q_b) located on the product side.

$$T_{mfp} = \frac{1}{kT}\int_{q_o}^{q_b} R(q') \exp\left(\frac{W(q')}{kT}\right) dq' \int_{q_a}^{q'} \exp\left(\frac{-W(q'')}{kT}\right) dq'', \qquad (4)$$

where q_a is a reflecting barrier upstream from q_o (Sigg et al., 1999).

Transition rate constants of the four-state DSM model were cast in the form, $a_{ij} = a_{ij}^o \exp[-(W_{ij} - q_{ij}V)/kT]$. The quantity a_{ij}^o is a pre-exponential factor, and W_{ij} and q_{ij} are the trough-to-peak activation energy and charge displacement, respectively. The kinetics of DSM models are obtained from solving the master equation:

$$\frac{d}{dt}\mathbf{P}(t) = \mathbf{P}(t)\mathbf{A}, \tag{5}$$

where the matrix $\mathbf{P}(t)$ contains transition probabilities $p_{ij}(t) = p(j,t|i,0)$, and $\mathbf{A}$ is the transition rate matrix whose elements are given by $\{a_{ij} - \Sigma_k a_{ik}\delta_{ij}\}$. Gating currents are readily computed via the following expression:

$$i_g(t) = \sum_r \langle \mathbf{p}_o \mathbf{v}_r \rangle \langle \mathbf{u}_r \mathbf{q} \rangle \lambda_r \exp(\lambda_r t), \tag{6}$$

where $\mathbf{v}$ and $\mathbf{u}$ are right and left eigenvectors of $\mathbf{A}$ with corresponding eigenvalues λ, $\mathbf{q}$ is a vector that contains the gating charge displacement for each state, and $\mathbf{p}_o$ is the state probability vector at time zero. Brackets ($\langle\,\rangle$) denote the vector inner product evaluated over all states. If the system has reached equilibrium under the resting potential V_r, the initial probability vector $\mathbf{p}_o$ is equivalent to $\mathbf{u}_o(V = V_r)$, where $\mathbf{u}_o$ is the left eigenvector corresponding to the 0^{th} eigenvalue ($\lambda_o = 0$). Eq. 6 can also be used to compute gating currents from a one-dimensional diffusion landscape if a suitable discretization scheme is used. These and additional details on computing the gating current variance and the problems of sampling and filtering are found in Sigg et al. (1999).

Monte Carlo simulations were performed by using the Langevin equation to simulate trajectories of x_g and x_b:

$$\frac{dx_g}{dt} = \frac{-\left(\frac{\partial W_{g,b}}{\partial x_g}\right)}{f_g} + \sqrt{\frac{2kT}{f_g}}\xi_g(t),$$

$$\frac{dx_b}{dt} = \frac{-\left(\frac{\partial W_{g,b}}{\partial x_b}\right)}{f_b} + \sqrt{\frac{2kT}{f_b}}\xi_b(t), \tag{7}$$

where ξ_g and ξ_b are uncorrelated, white, standard Gaussian noise sources. In practice, implementation of Eq. 7 was performed using a Euler algorithm with the Wiener process as the noise term. Simulations were initiated from the equilibrium distribution of the resting potential, and allowed to run at the test potential using a time step of 10^{-5} ms. Data were filtered and sampled during run time as described in Sigg et al. (1999). We used a random number generator with a long period ($>2 \times 10^{18}$, subroutine *ran2*; Press et al., 1992).

Electrophysiology

Shaker gating currents were measured with the cut-open oocyte vaseline gap technique (Stefani et al., 1994) at room temperature. Currents were recorded from *Xenopus* oocytes 2–5 days after injection with non-inactivating *Shaker* IR W434F cRNA (Perozo et al., 1993). W434F is a pore mutation that minimizes ionic currents but apparently does not affect activation kinetics (however, return charge movement is slowed down; see Yang et al., 1997). Solutions were composed of nonpermeant ions: internal, 120 mM *n*-methylglucamine(NMG)-methanesulfonate(MES), 1 mM K_2EGTA; and external, 120 mM NMG-MES, 2 mM $CaCl_2$. Solutions were buffered to pH 7.0 with 10 mM 4-(2-hydroxyethyl)-1-piperazineethanesulfonic acid (HEPES). Linear capacity currents were subtracted with the P/−4 technique (Bezanilla and Armstrong, 1977). Gating currents were acquired at 50-μs intervals and filtered at 5 kHz with an eight-pole Bessel filter. Details are found in Stefani et al. (1994). The SCoP v. 3.5 curve fitting program (Simulation Resources, Redlands, CA) with incorporation of custom solvers was used to simulate *Shaker* gating currents using a tetrameric form of the subunit model (see Results).

RESULTS

Construction of the single subunit model

Our initial goal was to create a minimal physical model with interacting two-state particles that could produce a rising phase in i_g. Our strategy favored an activation sequence consisting of, in this order: a long dwell time; a small charge movement; a shorter dwell time; and a large charge movement. In our two-particle subunit model, this corresponds to an initial inward translocation of the barrier particle followed by the outward transition of the gate particle (pathway C1→C**2**→C4 in Fig. 3). This pathway is favored if the gate particle is initially discouraged from leaving its resting position due to a large energy of activation, leaving the barrier particle to activate first. Relaxation of the barrier particle coordinate lowers the barrier seen by the gate particle due to electrostatic interaction, and the transition of the latter follows shortly. The alternate sequence C1→C**3**→C4 takes place also, but as it contributes a purely decaying term to the gating current, efforts were aimed at minimizing its occurrence.

In assigning values for the many degrees of freedom in our model we sought a degree of physical plausibility in the values of the charge valences z_g and z_b, the dielectric constant K, and the overall geometry. The process was done by trial and error, using the overall energy landscape (Fig. 2 *A*) and the shape of the gating current to guide our choices. We assumed a protein thickness of 25 Å. The energy landscapes of the individual gating particle were offset so that the permissive states of the oppositely charged gating particles were in close proximity (state C4). The mutual interaction between gating particles that occurs during activation produces positive cooperativity, which is necessary in generating a rising phase in the gating current. The interaction energy between the gating particles is a function of the protein dielectric constant (K), which we assumed was a static value. Using a reasonable separation distance of 5 Å between the lines of motion of the two gating particles, a rather large dielectric constant ($K = 30$) was needed to

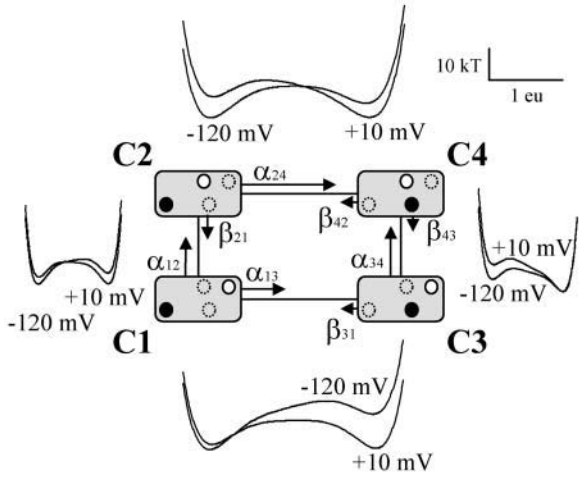

FIGURE 3 DSM representation of the single subunit model. PMF landscapes evaluated for individual transitions are shown for resting (−120 mV) and test (+10 mV) potentials. Transition arrows illustrate relative magnitudes of rate constants at +10 mV, but are not drawn to scale.

reduce the otherwise overwhelming electrostatic interaction energy. The valence of the gate charge was set at three electronic units (eu) to correspond to the number of significant gating charges in the S4 trans-membrane domain in *Shaker* (see Discussion). Assigning a valence of 2 eu to the barrier charge led to an overall gating charge displacement of $\sim$3 eu ($q_{12} + q_{24}$, see Table 2), which is about one-fourth the total gating charge per complete channel (four subunits) observed in *Shaker*. In reality, gating charge is spread over a larger volume—rather than in two point charges, as in our model—and so a smaller effective dielectric coefficient probably exists in ion channels. The energy landscape U_g required a large voltage offset ($V_g = 110$ mV) to prevent the gate particle from achieving the permissive state too easily, due to the attractive pull of the barrier particle. Thus, in the absence of an applied potential ($V = 0$ mV), U_g appears to favor the nonpermissive state (Fig. 1). But, if one considers the influence of the barrier particle on the gate particle by constructing a PMF profile with respect to q_g (Fig. 3), it is clear that the configuration of the gate particle with the lowest free energy is that of the permissive state. Given the above constraints, the combined range of values that fulfilled our criteria for a realistic appearing gating current were actually quite small, so it was not particularly surprising that there was not a dramatic variation in the value of fitted parameters obtained when simulating experimental data from *Shaker* (Table 1). The most notable exceptions are the values for f_g and V_g, which, as discussed in Methods, are inversely related when considering barrier transitions. Later, we shall see that there exists at least one other local minimum in the fitted parameter space, which could be discounted due to physical arguments. At this time, it is not possible for us to assign a global minimum due to the large number of fitted parameters and the restricted data set.

TABLE 2 Derived DSM variables

	Single subunit model			*Shaker* simulation
Variable	$V = -120$ mV	$V = 0$ mV	$V = 10$ mV	$V = 0$ mV
α_{12} (kHz)	0.038	0.41	0.48	0.77
β_{21} (kHz)	0.85	0.10	0.081	0.23
q_{12} (eu)	0.91	0.92	0.92	0.83
x_{12} (eu)	0.68	0.38	0.37	0.37
α_{24} (kHz)	0.022	1.99	2.68	2.57
β_{42} (kHz)	1.43	0.0074	0.0044	0.041
q_{24} (eu)	2.03	2.04	2.03	1.74
x_{24} (eu)	0.55	0.34	0.32	0.34
α_{13} (kHz)	0.00015	0.10	0.16	0.21
β_{31} (kHz)	6.82723†	0.087	0.053	0.19
q_{13} (eu)	2.10	2.18	2.18	1.85
x_{13} (eu)	0.75	0.57	0.54	0.57
α_{34} (kHz)	2.16	8.05756†	8.96717†	8.16422†
β_{43} (kHz)	0.069	0.0084	0.0075	0.043
q_{34} (eu)	0.86	0.74	0.72	0.65
x_{34} (eu)	0.26	0.056	0.033	0.018
α_{co}				10 ± 1*
β_{oc}				0.26 ± 0.02*
q_{co}				2.51 ± 0.07*
x_{co}				0.01 ± 0.0004*

*Fitted variables (mean ± SD).
†Adjusted for detailed balance.

Reduction to a discrete state Markov model

We took advantage of the hilly energy landscape to partition the activation pathway into four major transitions that take place over the saddle point areas (Fig. 3). We computed inverse transition rate constants as the mean first passage times across a PMF computed with respect to the activating particle, as outlined in Methods. This approximation proved quit serviceable; the accuracy increases with the height of the energy barrier—a useful property insofar as the rate-limiting step of a process figures heavily into the overall rate. One gauge of the correctness of the method is the ability to satisfy detailed balance. For any loop such as C1↔C2↔C4↔C3↔C1, the product of the rate constants in the clockwise direction must be equal to the product of the rate constants in the counterclockwise direction. The ratio of the two products for −120 mV is close to unity (1.0016), although a 25% discrepancy exists at 10 mV (likely due to overestimation of rate α_{34} due to loss of activation barrier height in transition C3→C4). To maintain detailed balance (necessary to ensure that gating currents decay to zero), we adjusted the largest rate constant before continuing with our calculations.

Table 2 lists rate constants computed for the subunit model at potentials −120 mV, 0 mV, and +10 mV. At the resting potential of −120 mV, the likelihood that a trajectory begins in state C1 is 95.6%. From this subensemble, $\phi_2 = 74.2\%$ of trajectories ultimately arrive in C4 via path C1→C**2**→C4 (percent value obtained by analyzing probability flow from C1 with an absorbing state located at C4), whereas the remainder $\phi_3 = 25.8\%$ use pathway C1→C**3**→C4. The likelihood of the first transition out of C1 being C1→C2 has nearly the same value (0.1635/(0.1635+0.4804) = 74.6%) as the frequency of the C1→**C2**→C4 pathway, signifying that, at +10 mV, return crossings back into C1 once the state has been vacated are improbable. The reason why the C1→**C2**→C4 pathway is approximately 3× more probable than the C1→**C3**→C4 pathway at 10 mV is evident from inspection of the energy landscape in Fig. 2 *A*. Despite larger frictional forces, the barrier particle must surmount a lower energy barrier out of state C1, and thus it is often the first to move. Rapid activation of the gating particle follows, and after many such trajectories, a rising phase in the cumulative gating current takes shape.

Monte Carlo analysis

As a check on the validity of the four-state DSM approximation and the accuracy of rate constant calculations, we acquired an ensemble of Monte Carlo trajectories using

the same voltage protocol and filtering characteristics applied to the numerical analysis. A sample trajectory superimposed onto the energy landscape is shown in Fig. 2 *A*. It demonstrates the sequence of the most probable activation pathway C1→C**2**→C4. The time course of the constituent particles during this trajectory is shown in Fig. 4. Of note is the (bandwidth-limited) abruptness of the transitions on the millisecond timescale and the positive concordance between the positions of gating and barrier particles in state C4. The disparity in the size of the two charge movements is evident from the differing heights of the transition spikes in the gating current. The ensemble mean of the Monte Carlo simulation and the numerical result obtained from the reduced model of Fig. 3 (for which kinetic parameters are listed in Table 1) are superimposed in Fig. 5. On the slow timescale, the agreement is satisfactory, and both methods predict a rising phase. Inspection of the Monte Carlo simulation reveals an additional fast component of i_g (reproduced with expanded bandwidth in the inset of Fig. 5); it arises from rapid equilibration in state C1 after depolarization. The decay time constant of the fast component is 170 ns, ~50× briefer than what has been observed in *Shaker* (Stefani and Bezanilla, 1996). This discrepancy is due to the small value of R_g. As we explained in Methods, the value of R_g is to some extent arbitrary because of the tradeoff with the free energy of activation. However, increasing f_g and f_b to a value that would slow the fast transient to the experimental value would also reduce activation barriers to unacceptable levels (near kT). Careful measurements of the voltage and temperature dependence of the fast transient have been performed to investigate this problem, the results of which will be presented in a later article. In short, a one-dimensional cross section of state C1 appears to undergo a reduction in the value of R from a rather large value in the diffusive portion of the C1 trough, to one that is comparable to the value of R_g before the first barrier transition.

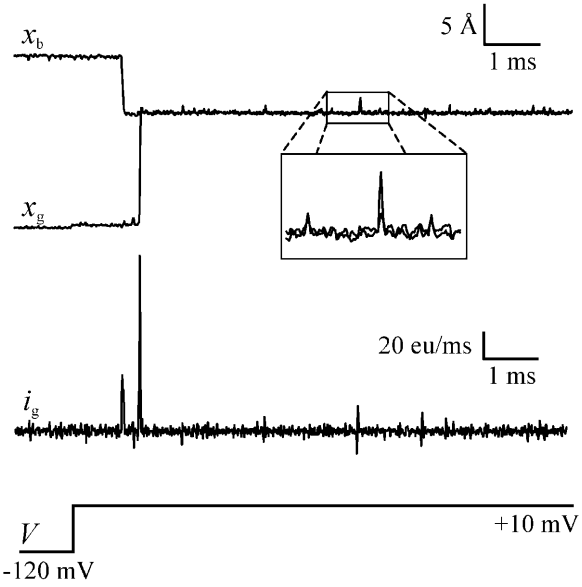

FIGURE 4 Time course of single subunit Monte Carlo trajectory shown in Fig. 2. Particle fluctuations (x_b, x_g) are in upper panel with the resultant gating current (i_g) shown underneath. $T = 291$ K; $f_c = 20$ kHz. The voltage protocol is displayed below.

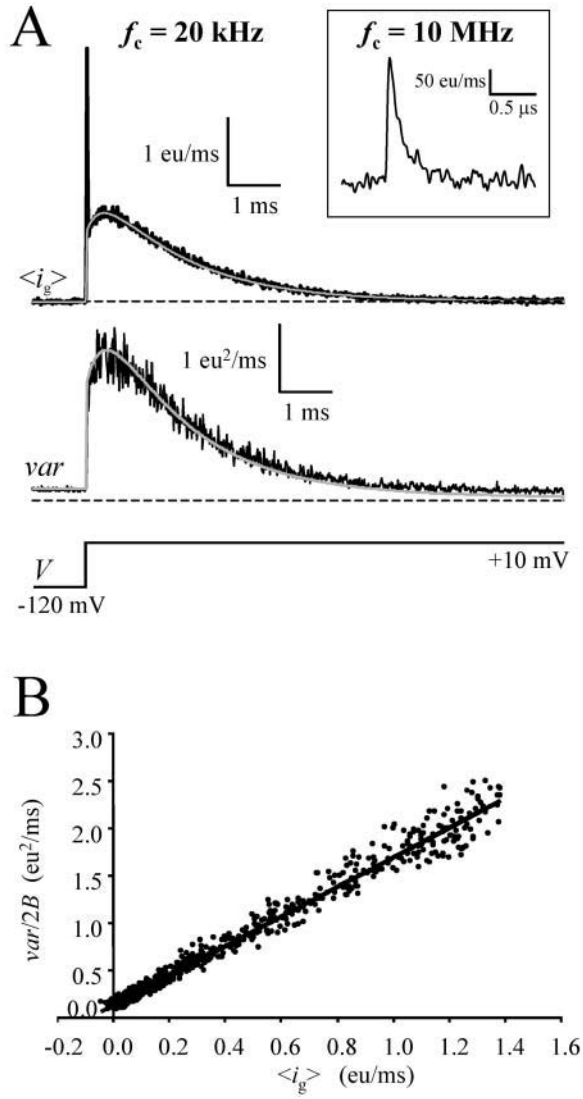

FIGURE 5 Ensemble gating current mean, $\langle i_g \rangle$, and variance, *var*, of a single subunit computed from 24,500 Monte Carlo trajectories. (*A*) Numerical predictions using the reduced DSM representation are shown as smooth tracings in gray. The dashed lines indicate a value of zero. An ensemble mean (17,900 runs) of the fast transient at high bandwidth (10 Mhz) is shown in the inset. (*B*) Plot of $var(t)/2B$ versus $\langle i_g(t) \rangle$ at 10 mV. Included are all data points shown in *A* after the fast spike. A least-squares fit (*straight line*) to the equation $var/2B = \Delta q_e \times \langle i_g \rangle + b$ yielded $\Delta q_e = 1.57$ eu and $b = 0.13$ eu²/ms.

The ensemble variance of the Monte Carlo current trajectories and the numerically derived gating current variance (obtained from an expression similar to Eq. 6; see Sigg et al., 1999) are superimposed in the lower panel of Fig.

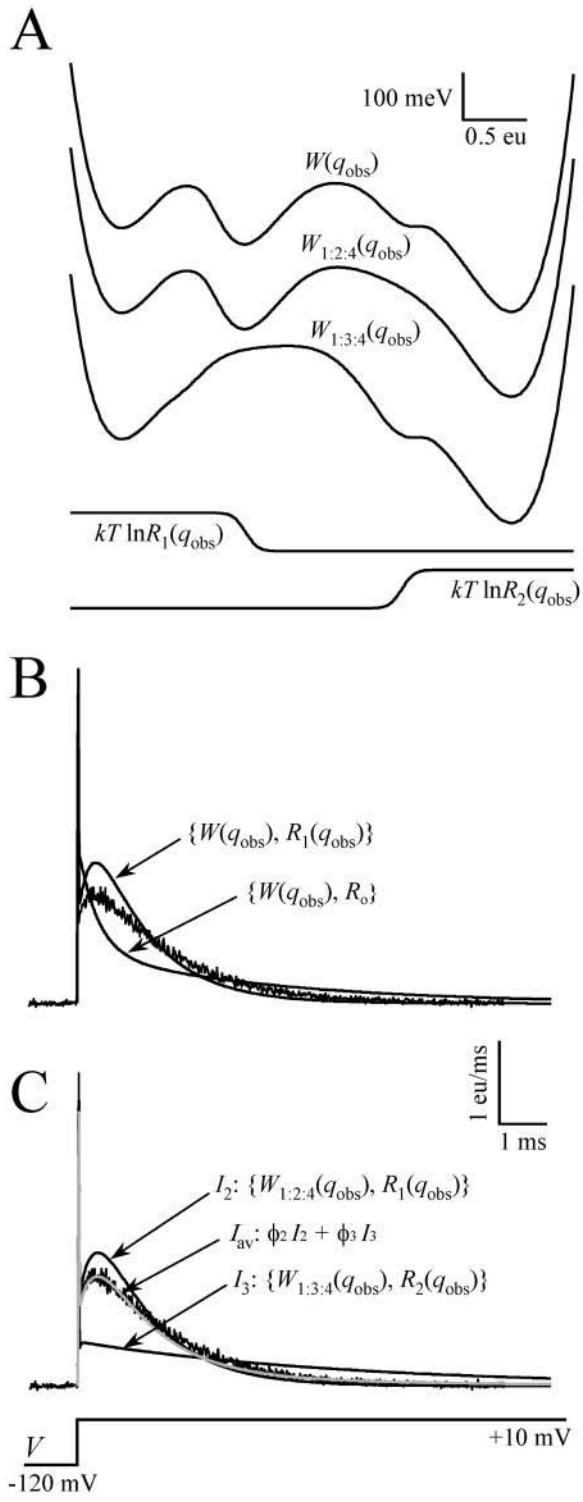

FIGURE 6 Predictions of $i_g(t)$ for reduced one-dimensional energy landscapes. (*A*) PMFs were obtained by applying Eq. 2 with respect to q_{obs} over different pathways: $W(q)$, integration over all space; $W_{1:2:4}(q)$, integration over upper activation pathway; and $W_{1:3:4}(q)$, integration over lower activation pathway. These free energy pathways were combined with inhomogeneous resistance landscapes, drawn in the form of an effective potential $kT\ln R$: $R_1(q)$ changes from $R_g = 11.25$ to $R_b = 0.444$ ms × mV/eu; $R_2(q)$ from R_b to R_g. R_o is a constant value of resistance arbitrarily set at 5 ms × mV/eu. (*B*) Monte Carlo simulation (same as Fig. 5 *A*) superimposed onto 5 *A*. The large value of the peak variance and the varying time course arise from transition-generated shot noise, a feature seen also in *Shaker* (Sigg et al., 1994) as well as the sodium channel (Conti and Stühmer, 1989). The so-called elementary charge movement Δq_e is a measure of the largest gating charge movement along the activation pathway, and is defined as the slope of *var*/2*B* versus *i*g, where B is the system bandwidth (= 1.064 × the cutoff frequency of a Gaussian filter). A rough estimate of Δq_e is given by $\Sigma q_i^2/\Sigma q_i$ (Conti and Stühmer, 1989), which for the C1→C**2**→C4 pathway has the value 1.68 eu, similar to the simulated value of 1.57 eu obtained from Monte Carlo trajectories (Fig. 5 *B*). The Monte Carlo simulations demonstrate that general features of experimental recordings from actual ion channels can be reproduced with the subunit model; these include nonstationary shot noise and the existence of separate timescales in the gating current—all characteristics of a hilly energy landscape. Similarities such as these lend credence to the notion that such a landscape is a useful tool in modeling gating kinetics (Sigg et al., 1999).

Reduction to one-dimensional landscapes with sequential transitions

As an alternative to the DSM representation, we reduced the subunit model to one or two single-dimension PMF landscapes (Fig. 6). The results retain diffusion kinetics and predict both fast (intrastate) and slow (interstate) kinetics. We initially chose a free energy landscape with respect to q_{obs}, the measurable gating charge, where the range of integration covers the entire phase space. $W(q_{obs})$ has two prominent barriers (Fig. 6 *A*), which roughly correspond to the transition of the ''barrier'' particle, followed by the movement of the gate particle (path C1→C**2**→C4). The advantage of using q_{obs} as the reaction coordinate is its direct relationship to voltage clamp data, and because it encompasses the individual particle charge displacements q_b and q_g, it is a reasonable choice for a global reaction coordinate. Despite these advantages, $W(q_{obs})$ did not reproduce the mean gating current computed from Monte Carlo trajectories (Fig. 5 *B*). $W(q_{obs})$ combined with an arbitrary constant value of the resistance R failed to produce a rising phase at all. By varying the resistance according to what particle is dominating the PMF (this was done by changing the value of the resistance from R_b to R_g after the first barrier jump; R_1 in Fig. 6 *A*), we succeeded in generating a rising phase but failed to numerical predictions of gating currents employing combinations of PMF and resistance landscapes. Combining $W(q)$ with either constant (R_o) or variable ($R_1(q)$) resistance led to poor estimates of the Monte Carlo time course (*upper panel*). (*C*) The most faithful reproduction is a weighted average (I_{av}) of currents predicted by upper (I_2) and lower (I_3) activation pathways (*lower panel*, in *gray*). The weights, $\phi_{\mathbf{2}} = 0.748$, and $\phi_{\mathbf{3}} = 0.258$, are splitting probabilities for the paths C1→C**2**→C4 and C1→C**3**→C4, respectively.

match the expected time course of $i_g(t)$.

To produce a reasonably accurate facsimile of the gating current, the following procedure was used: PMFs with respect to q_{obs} were obtained for individual pathways of the activation landscape, namely C1↔C**2**↔C4 and C1↔C**3**↔C4 (Fig. 5 *A*). Gating currents were predicted in each case and a weighted average based on frequency of occurrence (roughly 3:1, as evaluated earlier) was obtained. The result, shown in Fig. 5 *C*, failed to match the accuracy of the DSM predictions, but was nonetheless a close approximation to the ensemble mean of Monte Carlo trajectories, particularly during the rising phase portion of the curve. Thus, reduction to one-dimensional PMF landscapes can be used to calculate fast and slow gating currents if one performs the following: vary the resistance according to what particle exerts the greatest influence over a region of the PMF landscape, and construct the gating current from a weighted sum of contributions from all possible pathways. The effort needed to define a variable resistance landscape, combined with questionable accuracy and more involved computations, make the one-dimensional landscape approach much less attractive in computing slow gating kinetics than reduction to a DSM model.

A key point that can be inferred from the preceding paragraph is that representation of many-particle systems cannot be reduced to the PMF of a single measurable reaction coordinate unless coupling between the major variables of activation is very strong. It follows that linear models of activation cannot be assumed; they must be proven.

Curve fitting with a tetrameric model

Having achieved reasonably appearing gating currents using a single subunit model, we next decided to combine four identical subunits in the manner of a ZHA-like model and attempted to curve-fit gating currents obtained from *Shaker*. We included a final opening step to facilitate fitting of return (*OFF*) currents, and to add extra charge to the activation sequence. Because there is significant representation of both the C1↔C**2**↔C4 and the C1↔C**3**↔C4 pathways in a single subunit, the convolution of four such schemes (Fig. 7) requires a greater number of states (36 total) when compared to similar so-called 2 + 1 models (16 states) that appear in the literature. Apart from the final opening step, the model is identical to the type E-model considered by Zagotta et al. (1994). Due to the increased combinatorial complexity at this stage, we chose to dismiss possible subunit-to-subunit interactions and did not attempt to propose a physical mechanism for the concerted opening of the channel. Instead, we made the assumption that the permissive state for channel opening occurs in any state in which all gate and barrier particles are in their activated positions. We had considered the case in which only the positioning of the gate particles are required for opening. This leads to opening steps from all of the five states labeled by an asterisk in the expanded scheme shown in Fig. 8. However, due to our choice of model parameters, the lower four open states were rarely populated, and there was no significant change in the predicted ionic (or gating) current, so we used the simpler opening scheme, illustrated in Fig. 8.

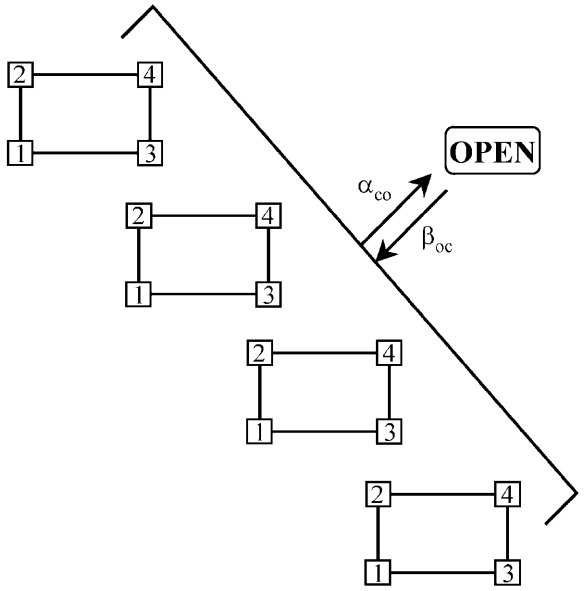

FIGURE 7 Schematic view of the DSM model used to simulate *Shaker*. Four single subunit models are linked at state C4, from which a concerted opening transition takes place.

The results of the fit are shown in Fig. 9 and Tables 1 and 2. The transition from one-exponent (−120, −60 mV) to two-exponent decay (−50 to −10 mV) of the activation (*ON*) current was faithfully reproduced, though the rising phase of the fit tracings are not as developed as in the data. The most glaring transgression of the model is in overestimating the *ON* decay rate at potentials greater than −30 mV. This might be corrected by adding an extra step in the subunit activation sequence, as was suggested by Schoppa and Sigworth (1998), though this would require the addition of a third gating particle. To fit the *OFF* current, a rather large charge (q_{co} = 2.51 eu) was used in the last (opening) step, the voltage dependence of which is derived entirely from the closing transition (x_{co} = 0.01). We recognize the insensitivity of our data set to transitions near the open state, as the *OFF* current was evaluated at only one potential. Patch clamp data of single channels have demonstrated that transitions from the open state move little charge (Hoshi et al., 1994; Schoppa and Sigworth, 1998). Thus, realistically, there should be an additional voltage-insensitive transition added to the end of the activation sequence in our model, but as we are more concerned here about earlier transitions, we will not pursue the matter further.

We placed no constraint on the maximal gating charge of activation per channel. Nevertheless, the fitted value of 12.8 eu is similar to published values in *Shaker* (Schoppa et al., 1992; Aggarwal and MacKinnon, 1996; Seoh et al., 1996).

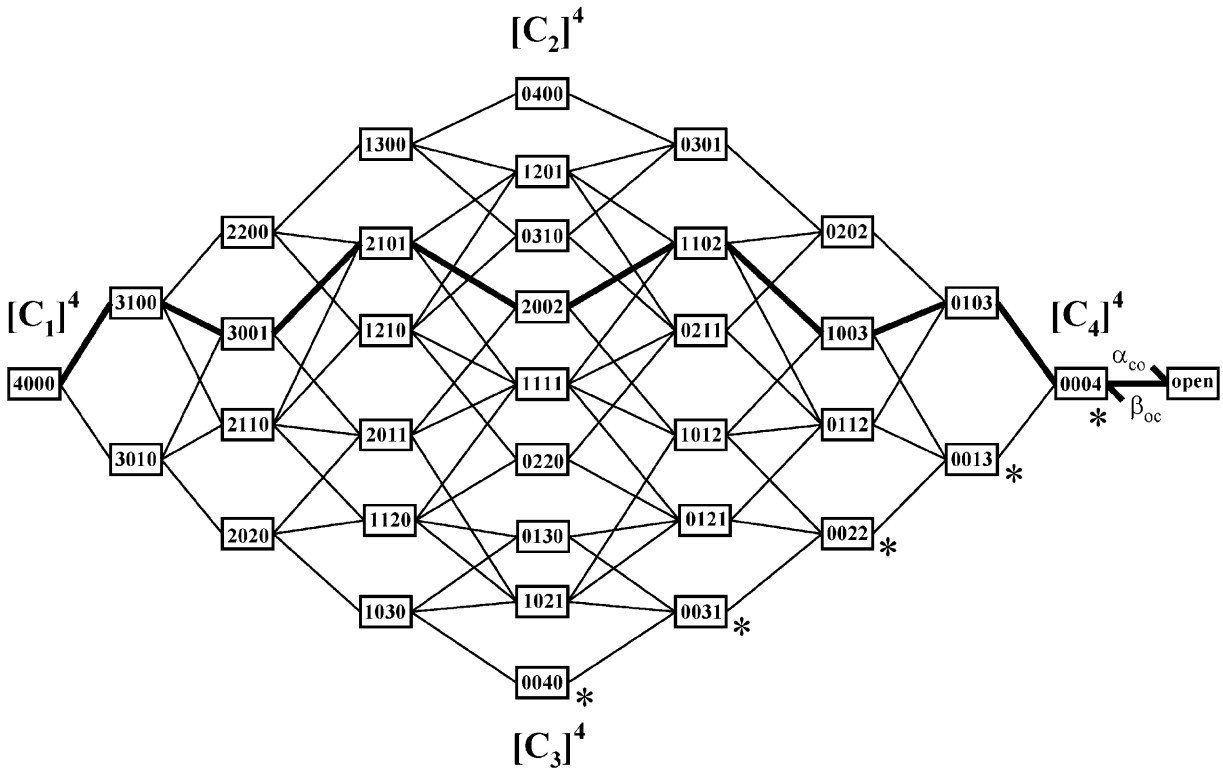

FIGURE 8 Expanded view of the DSM model in Fig. 6. Individual states (*boxes*) are characterized by their occupation numbers (subunits assumed to be indistinguishable) in the order [C1, C2, C3, and C4]. The heavy line is the most likely pathway of channel activation. Transition rate constants are obtained by 1), determining which transition occurred by detecting changes in occupation numbers; and 2), multiplying the rate constant for that transition by the occupancy number of the initial state. For example, the forward rate constants of the first two transitions on the heavy line are $4\alpha_{12}$ and α_{24}. States labeled with an asterisk (*) are those that would lead to an opening if the gate particle were the sole determinant of permissiveness to opening.

Not surprisingly, given the reasonable modeling of current tracings, the simulated voltage dependence of equilibrium gating charge displacement (Q-V plot) matches the experimental data fairly well (Fig. 9, *inset*).

DISCUSSION

A major objective of this work was to develop methods in computing electrophysiologically relevant kinetics from a physical model. Our benchmark for accurate dynamics was Monte Carlo simulation, which given a small enough time interval and a good random number generator, is exceedingly robust, but may take hours to days to obtain a sizeable number of trajectories. We succeeded in developing a speedier numerical method in the case of a two-particle system by reducing the hilly landscape into a four-state DSM model. Gating currents were then obtained using traditional methods. The key to a reliable implementation of this approach is to pair well-defined transition pathways with a proper choice of reaction coordinate. In our model, useful reaction coordinates were q_g for the C1↔C3 and C2↔C4 transitions, and q_b for the C1↔C2 and C3↔C4 transitions. A PMF with respect to the reaction coordinate was then obtained from Eq. 2, from which inverse rate constants can be reliably estimated as the mean first passage time across the transition barrier (Reimann et al., 1999). The method is readily extended to a larger number of degrees of freedom, and its main limitation is that it is restricted to barrier transition models. In cases where barriers are not large enough to derive meaningful rate constants, reduction to one-dimensional diffusion landscapes is an alternative option, though we found this method to be computationally more involved and less accurate (compare Figs. 5 and 6). However, it does have the advantage of being able to predict fast components of gating (Sigg et al., 1999).

Model considerations

In choosing a model, we attempted to strike a balance between simplicity of design and relevance to the perceived structure of potassium channels. The positively charged gate particle in our model is an evident reference to the S4 trans-membrane domain found in all voltage-sensitive channels. The lesser, negatively charged barrier particle could be interpreted as the *environmental influence* on the S4 segment. Candidates for residues that contribute to the barrier particle could include the negatively charged residues in the S2 and S3 domains, which, along with the

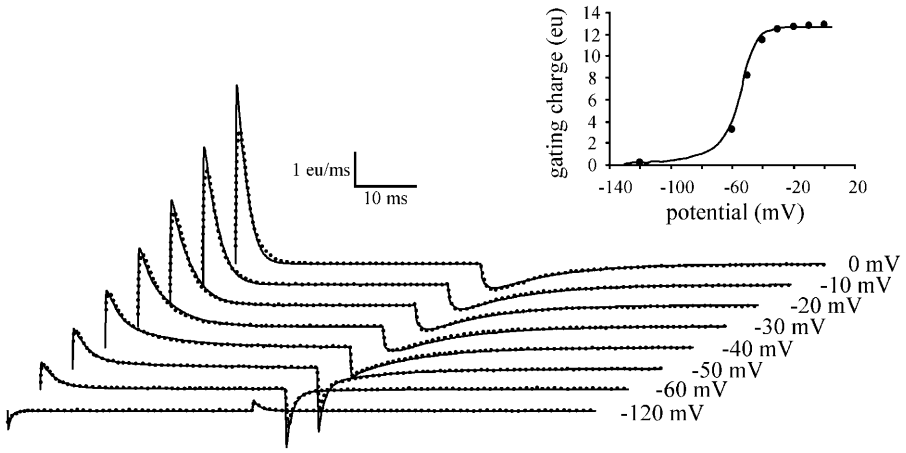

FIGURE 9 Curve fits of *Shaker* gating currents using the tetrameric model shown in Figs. 8 and 9. Data (*dots*) and fits (*smooth line*) are superimposed. Holding potential: −90 mV; $T = 291$ K; and $f_c = 5$ kHz. Test potentials are shown to the right of tracings. (*Inset*) Single channel Q-V plot. The smooth line is $\langle g(V)\rangle = \langle \mathbf{p}_\infty(V)\mathbf{q}\rangle$, computed from the model. Data points in circles were obtained from integrating *ON* currents and normalized to superimpose onto the model Q-V.

S4 segment, have been implicated as possessing a role in the gating process (Seoh et al., 1996). Our depiction of gating particles as point charges that move linearly across a uniform electric field is openly naïve, but it is better suited toward mathematical treatment than other more realistic scenarios such as helix tilts or rotations (for review see Horn, 2000; Sansom, 2000; Bezanilla, 2000). It should be emphasized that the essential features of the model involving charge displacement and barrier modification through interaction coupling are translatable to other geometries. In particular, the model is easily adapted to a system that has charged residues on an α-helix rotating from an internal water-filled crevice to an external crevice, as has been suggested for *Shaker* (Bezanilla, 2000; Starace et al., 1997). The local electric field would presumably be directed at nearly right angles to the helix, instead of along the membrane perpendicular. At the time of this writing, unequivocal evidence of channel structural information in the form of x-ray crystallography data is lacking, so for the sake of ease of visualization and as a means toward simplifying the mathematics, we chose the most straightforward geometry, that of direct translation.

Other features of the model deserve comment. The presence of invaginations, or vestibules, on both sides of the protein (see Fig. 1) appears similar to those theorized by Yang et al. (1996) and Starace et al. (1997) from accessibility studies, and by Islas and Sigworth (2001) from studying loss of total gating charge under hypotonic conditions. The similarity is not purely cosmetic, as the use of vestibules in our model enables directed focusing of the electric field across a variable distance, allowing the energy landscapes of the two gating particles to be offset in the x-direction without a concomitant reduction in sensitivity to the membrane potential. However, no attempt was made to solve the Poisson-Boltzmann equation to determine field lines, as was done in the work by Islas and Sigworth (2001). Instead, we assumed parallel lines everywhere with linear voltage drops that did not extend into the electrolyte solution. We also confined the gating particles to the protein dielectric without access to the internal or external solutions, although experimental evidence supports the notion of solvent accessibility of the charged residues that participate in gating. Again, this was done for the sake of mathematical convenience, to prevent discontinuities in the slope of the energy landscape. In fact, a realistic picture of gating would have the participating charges occupy an intermediate position between being ''buried'' in the protein matrix and completely dissolved in solution, so that it is unlikely that any one charged particle moves through the entire membrane field. In the case of the barrier particle, we purposely limited its range within the protein dielectric (see Fig. 1) as a way of reducing the gating charge for a given valence.

Origin of the rising phase

An interesting topic of speculation is why a rising phase is observed in the gating current of many voltage-dependent channels. In our model, it is generated by Coulomb interactions between a pair of two-state particles. Activation of the dominant gate particle is delayed until the barrier particle moves into position—a classic example of a non-Markovian transition. A similar mechanism, if it exists in nature, could be used to modulate the frequency of S4 transitions through subtle shifts in the surrounding environment. Such control might be useful in, among other things, controlling the rate of activation through the action of external divalents (more on this later).

We have up to this point neglected a model consisting of a lone gate particle undergoing a single non-Markovian transition, as a way of generating the rising phase in i_g (see Clay, 1995, for a similar idea). In this variation of our existing model, the gate particle continues to interact with its environment, but is now the sole contributor to the gating current. We experimented at some length with barrier modulation by a nongating but attracting particle fluctuating in a harmonic well, as a means of instilling time dependence into the gate particle transition rate. Although we failed at numerous attempts to achieve a rising phase through Monte

Carlo simulation with various incarnations of this basic idea, it remains in principle a viable one.

Features of the reduced Markov representation

A property of the reduced DSM version of our physical model that is different from conventional DSM models is the small voltage dependence of ordinarily invariant quantities. These include the transition charge displacements and relative locations of barrier peaks, as is evident from studying Table 2. Much of the latter is attributable to the flat top of the intrinsic particle energy profile. The effect is a migrating barrier peak as a function of voltage (Fig. 3); thus, we always recomputed DSM variables for every voltage. Even so, given sufficiently large barriers, extrapolation of model parameters from the values obtained at an intermediate potential yields gating currents that are not tremendously different than if the DSM variables had been computed from the test potential. This is not a generalization, however, and one must be cautious about defining a reduced DSM model with respect to its components evaluated at a single voltage.

Properties of the fast transient

The fast gating current transient is a feature of diffusion gating that has been experimentally recorded in the squid axon sodium channel (Forster and Greeff, 1992), and in the *Shaker* potassium channel (Stefani and Bezanilla, 1996). Calculating the gating current using an energy landscape representation of the subunit model, we see the typical spike arising from rapid intrastate re-equilibration that precedes the slow components of the gating current. It is of significant interest to know whether the fast transient in our model can be resolved under experimental conditions, where the presence of a large linear membrane capacity transient requires subtraction methods to uncover the nonlinear gating component. This is done by employing different holding potentials for the test and subtraction protocols (we define here a holding potential as the voltage at which the membrane is held for long enough that the gating current transients in the time frame of interest have died out). The subtraction pulse protocol must occur outside the range of voltage that moves gating charge (Bezanilla and Armstrong, 1977). In *Shaker*, It has been experimentally shown that the shape of the fast gating transient is independent of the subtraction protocol used as long as the subtracting holding potential is greater than 0 mV and the direction of the subtraction step is positive (data to be published). This implies that the potential minimum populated at positive potentials (i.e., the open state) is quite narrow and deep compared to closed states populated by negative holding potentials. We wondered if, in the present model, whether the mutual interaction between gate and barrier particles in their permissive (activated) states would be enough to noticeably narrow the width of the energy trough in state C4 relative to state C1—enough to record a difference in the fast transient after a rapidly depolarizing potential. A quick glance at Fig. 2 suggests only subtle differences in trough shape between state C1 at −120 mV and state C4 at +10 mV. Nevertheless, we tested for a difference in fast transients at these two potentials with high bandwidth Monte Carlo simulations, comparing fast transients for a pulse from −120 to +10 mV (test protocol) and one from +10 mV to +140 mV (subtraction protocol). There were only slight differences in the transients, resulting in a small difference current whose amplitude was in the opposite direction of what was expected! We concluded that electrostatic interactions of the type we used in our model are not sufficient to generate an experimentally observable fast transient. What is needed is for the gating structure of the channel to be dramatically inflexible at the end of the activation sequence, likely as a result of the concerted transitions into the open state—through a mechanism yet to be determined.

Modeling the *Shaker* channel

In fitting our model to *Shaker* gating currents, we gravitated fairly quickly toward a tetrameric model with one additional concerted opening state (2 + 1 scheme). In this way we had more flexibility in adjusting for *ON* and *OFF* characteristics. We initially tried modeling with a single subunit and, surprisingly, achieved an excellent fit of the *ON* and *OFF* gating currents at +10 mV with a holding of −90 mV. However, this came with the price of a reversal in the intended activation sequence (discussed below), and increasingly poor fits with negative test potentials.

Fits using the 2 + 1 scheme resulted in a gating charge displacement of 1.74 eu for the gate transition C2↔C4. Although not excessively large, this charge movement is nevertheless responsible for the rapidly increasing *ON* decay that constitutes the primary failure of the model. Due to the relatively low transition barriers at $V = 0$ mV (3.2 kT for transition C1↔C2 and 4.7 kT for transition C2↔C4), we hoped that as the transitions became diffusion-limited, their rates would be overestimated by the mean first passage time approximation. This turned out not to be the case, however, as Monte Carlo simulation of an individual subunit matched the expected DSM prediction exceptionally well. Reconciling the need for smaller voltage dependence of the *ON* current with the well-documented measurements 12–13 eu of essential gating charge movement might require at least three or more transitions in the subunit pathway, as discussed by Schoppa and Sigworth (1998). Going over into a diffusion process with a large number of transitions is not an option, however, as it would carry the fast transient into the slow timescale. Shot noise in the early transitions would also be markedly decreased, although the fitted value of 2.51 eu for the gating charge q_{co} moved in the concerted, final opening step is itself large enough to account for the late charge

movement inferred by Sigg et al. (1994) from gating current noise analysis.

Experimental evidence for charge interactions in K^+ channels

A model of charge rearrangements that bears a resemblance to our scheme, involving positively charged *Shaker* residues R368 and R371 in the S4 segment and the negatively charged E283 in the S2 segment, has been proposed on the basis of accessibility studies combined with charge reversal experiments (Tiwari-Woodruff et al., 2000). They theorize that interactions between the S2 and S4 segments occur near the permissive state of an individual subunit, rather than in the most closed state. A similar interaction occurs between the barrier and gate charges in the present subunit model. Differences in the two models include an intermediate state in the S4 activation sequence of their model, whereas all gating particles in the subunit model fluctuate between only two states. Also, charge neutralization experiments suggest that the negatively charged residue E283 does not sense the membrane field (Seoh et al., 1996), a fact that is reflected in it remaining stationary in their model. Thus, although charge interactions in the permissive state occur in both schemes, the results of the accessibility studies imply a different origin of the rising phase, that of two-step activation of the S4 segment, rather than the preferential sequence of two-particle activation that exists in the model entertained here.

A second charge network in *Shaker*, involving negative charges in the S2 (E293) and S3 (D316) segments, and the positively charged K374 residue in the S4 segment, was discovered using second-site mutational analysis to rescue detrimental charge neutralizations (Papazian et al., 1995). Although the role of this charge network in gating dynamics has yet to be clarified, neutralization of one of the negative charges, E293, actually reduces overall charge movement significantly. E293 is the only negative charge in *Shaker* for which this has been convincingly shown (Seoh et al., 1996). It was proposed that E293 interacts with the S4 segment in the most closed state (Papazian and Bezanilla, 1999), prompting us to wonder if a rising phase in the gating current can arise from an alternative starting point—one in which the gating particles are initially in close proximity. The role of the barrier particle is changed from encouraging activation of the gate particle to hindering it through electrostatic binding. Once it has moved away, however, the gating particle is free to make a transition. The sequence of activation can in principle remain unchanged. We tested this possibility by simply fitting the single subunit model to the *OFF Shaker* gating current with a pulse from +10 to −90 mV. A successful fit implies that a starting point with both gating particles in the permissive position can lead to a rising phase. As mentioned earlier, we obtained quite a good fit to *ON* and *OFF* currents for this voltage protocol. Interestingly, in the setting of a fixed geometry that we imposed onto the model, there was a reversal in the sizes of gating charge valence, so that now $|z_b| > |z_g|$. Also reversed was the activation sequence of particles. The gate particle was more likely to activate first, in essence being delegated to the role of barrier particle. We attempted to use this new scheme in fitting the full *Shaker* activation series of gating currents to the tetrameric construct of the model, achieving a slightly better fit than with the original ($\chi^2 = 13.7$ vs. 15.9)—thus demonstrating for the present model that there is no unique set of parameters that will simulate *Shaker* gating, and that other considerations are needed. In this case, the relatively smaller-sized valence of the positive charge makes the alternative model a less realistic one.

An intriguing set of results found in another potassium channel, the ether-à-go-go (eag) channel, has possible relevance to the present mechanical model. The gating current of eag, which like *Shaker* exhibits a rising phase, is slowed by the presence of external Mg^{+2} binding in a water-filled crevice between the S2 and S3 transmembrane segments (Tang et al., 2000; Silverman et al., 2000). The effects of Mg^{+2} binding in eag could be explained in a ZHA-like model by a decrease in both forward and reverse rates of the first subunit transition, and the forward rate of the second subunit transition (Tang et al., 2000). In the context of the present mechanical model, this behavior could be explained if the magnesium ion binds to a site directly on or near the barrier particle, reducing its effective valence. Steric hindrance or mass effects might slow down fluctuations in the motion of the barrier particle-Mg^{+2} complex, leading to a reduction of rates across the first subunit transition. At the same time, a weak electrostatic interaction between the pair of gating particles hinders the ability of the gate particle to activate, causing the forward rate of the second subunit transition to be reduced. If such an interaction between the magnesium ion and the presently proposed gating structure exists, it would be a worthy example of how modulation of channel activation by environmental influences could be achieved through the action of a barrierlike moiety.

CONCLUSION

We have proposed a simple mechanical model of a potassium channel whose slow dynamics can be rapidly evaluated to generate gating currents. Though crude, the model predicts gating currents that are similar to those recorded in *Shaker* and other potassium channels. Several features of the model are quite novel, such as the partial coupling of two gating particles as the source of the rising phase in i_g, and the use of mechanical variables to describe the model such as position, valence, and force (but see also Levitt, 1989). One feature that is not novel, but has lately fallen out of favor, is the two-state nature of the individual gating particles (Hodgkin and Huxley, 1952). Given recent studies that demonstrate accessibility of gating residues to both external and internal environments, it is not unreasonable to theorize that a gating

particle such as the S4 trans-membrane domain prefers conformations that position its charges near an electrolyte solution, and that these charges (which, if the S4 is an α-helix, are in close alignment) might flit back and forth across the energetically inhospitable protein matrix—in other words, behave like a two-state particle.

The numerical techniques used here can be generalized to more involved systems with increasing number of particles and different geometries, so long as the n-dimensional energy landscape is reducible to well-defined, one-dimensional transition pathways. Although the present model was developed heuristically, it is hoped that once the crystal structure of a voltage-gated potassium channel is available, similar methods can be used to test the dynamic properties of the channel in terms of its electrophysiological properties.

Note added in proof: Shortly before publication of this article the crystal structure of a voltage dependent bacterial K^+ channel was made available (Jiang et al. 2003. *Nature*. 423:33–41). Accessibility studies with the crystal structure in mind (Jiang et al. 2003. *Nature*. 423:33–41) suggest that gating charges on a hinged S3-S4 ''paddle'' experiences a 15 to 20 Å translation across a hydrophobic interface (the plasma membrane—contrary to prior conventional wisdom, which had the S4 imbedded inside the protein matrix). In addition, movement of the S2 segment appears possible, as it is loosely attached to the rigid pore in the model put forth by the authors. Thus, the mechanism for S4 modulation by external influences such as the S2 segment proposed here is not inconsistent with their data; though it remains to be tested—and shown that this interaction is responsible for the rising phase in the gating current.

We thank Dr. John Bannister for stimulating discussion, and Dr. Rikard Blunck for devising a pleasing composition for the state diagram in Fig. 8.

Supported by National Institutes of Health grant GM30376 (to F.B.), and training grant in Cellular Neurobiology NS07101 (to D.S.).

REFERENCES

Aggarwal, S. K., and R. MacKinnon. 1996. Contribution of the S4 segment to gating charge in the *Shaker* K^+ channel. *Neuron*. 16:1169–1177.

Bao, H., A. Hakeem, M. Henteleff, J. G. Starkus, and M. D. Rayner. 1999. Voltage-insensitive gating after charge-neutralizing mutations in the S4 segment of *Shaker* channels. *J. Gen. Physiol.* 113:139–151.

Bezanilla, F., and C. M. Armstrong. 1977. Inactivation of the sodium channel. I. Sodium current experiments. *J. Gen. Physiol.* 70:549–566.

Bezanilla, F., and R. E. Taylor. 1982. Voltage-dependent gating of sodium channels. *In* Abnormal Nerve and Muscle as Abnormal Impulse Generators. W. Culp and J. Ochoa, editors. Oxford University Press, New York.

Bezanilla, F. 2000. The voltage sensor in voltage-dependent ion channels. *Physiol. Rev.* 80:555–592.

Clay, J. R. 1995. A simple model of K^+ channel activation in nerve membrane. *J. Theor. Biol.* 175:257–262.

Conti, F., and W. Stühmer. 1989. Quantal charge redistributions accompanying the structural transitions of sodium channels. *Eur. Biophys. J.* 17:53–59.

Forster, I. C., and N. G. Greeff. 1992. The early phase of sodium channel gating current in the squid giant axon. Characteristics of a fast component of displacement charge movement. *Eur. Biophys. J.* 21:99–116.

Hodgkin, A. L., and A. F. Huxley. 1952. A quantitative description of membrane current and its application to conduction and excitation in nerve. *J. Physiol.* 117:500–544.

Horn, R. 2000. A new twist in the saga of charge movement in voltage-dependent ion channels. *Neuron*. 25:511–514.

Hoshi, T., W. N. Zagotta, and R. W. Aldrich. 1994. *Shaker* potassium channel gating. I: Transitions near the open state. *J. Gen. Physiol.* 103:249–278.

Islas, L. D., and F. J. Sigworth. 2001. Electrostatics and the gating pore of *Shaker* potassium channels. *J. Gen. Physiol.* 117:69–89.

Kanevsky, M., and R. W. Aldrich. 1999. Determinants of voltage-dependent gating and open-state stability in the S5 segment of *Shaker* potassium channels. *J. Gen. Physiol.* 114:215–242.

Keynes, R. D., and F. Elinder. 1998. On the slowly rising phase of the sodium gating current in the squid giant axon. *Proc. R. Soc. Lond. B Biol. Sci.* 265:255–262.

Ledwell, J. L., and R. W. Aldrich. 1999. Mutations in the S4 region isolate the final voltage-dependent cooperative step in potassium channel activation. *J. Gen. Physiol.* 113:389–414.

Levitt, D. G. 1989. Continuum model of voltage-dependent gating. Macroscopic conductance, gating current, and single-channel behavior. *Biophys. J.* 55:489–498.

Mannuzzu, L. M., and E. Y. Isacoff. 2000. Independence and cooperativity in rearrangements of a potassium channel voltage sensor revealed by single subunit fluorescence. *J. Gen. Physiol.* 115:257–268.

Papazian, D. M., X. M. Shao, S. A. Seoh, A. F. Mock, Y. Huang, and D. H. Wainstock. 1995. Electrostatic interactions of S4 voltage sensor in *Shaker* K^+ channel. *Neuron*. 14:1293–1301.

Papazian, D. M., and F. Bezanilla. 1999. Voltage-dependent activation of ion channels. *Adv. Neurol.* 79:481–491.

Perozo, E., R. MacKinnon, F. Bezanilla, and E. Stefani. 1993. Gating currents from a nonconducting mutant reveal open-closed conformations in *Shaker* K^+ channels. *Neuron*. 11:353–358.

Press, W. H., S. A. Teukolsky, W. T. Vetterling, and B. P. Flannery. 1992. Numerical Recipes in C, 2nd Ed. Cambridge University Press, New York.

Reimann, P., G. J. Schmid, and P. Hänggi. 1999. Universal equivalence of mean first-passage time and Kramers rate. *Phys. Rev. E Stat. Phys. Plasmas Fluids Relat. Interdiscip. Topics*. 60:R1–R4 (Review).

Sansom, M. S. 2000. Potassium channels: watching a voltage-sensor tilt and twist. *Curr. Biol.* 10:R206–R209 (Review).

Schoppa, N. E., and F. J. Sigworth. 1998. Activation of *Shaker* potassium channels. III. An activation gating model for wild-type and V2 mutant channels. *J. Gen. Physiol.* 111:313–342.

Schoppa, N. E., K. McCormack, M. A. Tanouye, and F. J. Sigworth. 1992. The size of gating charge in wild-type and mutant *Shaker* potassium channels. *Science*. 255:1712–1715.

Seoh, S. A., D. Sigg, D. M. Papazian, and F. Bezanilla. 1996. Voltage-sensing residues in the S2 and S4 segments of the *Shaker* K^+ channel. *Neuron*. 16:1159–1167.

Sigg, D., H. Qian, and F. Bezanilla. 1999. Kramers' diffusion theory applied to gating kinetics of voltage-dependent ion channels. *Biophys. J.* 76:782–803.

Sigg, D., E. Stefani, and F. Bezanilla. 1994. Gating current noise produced by elementary transitions in *Shaker* potassium channels. *Science*. 264:578–582.

Silverman, W. R., C. Y. Tang, A. F. Mock, K. B. Huh, and D. M. Papazian. 2000. Mg^{+2} modulates voltage-dependent activation in ether-à-go-go potassium channels by binding between transmembrane segments S2 and S3. *J. Gen. Physiol.* 116:663–678.

Smith-Maxwell, C. J., J. L. Ledwell, and R. W. Aldrich. 1998. Uncharged S4 residues and cooperativity in voltage-dependent potassium channel activation. *J. Gen. Physiol.* 111:421–439.

Starace, D. M., E. Stefani, and F. Bezanilla. 1997. Voltage-dependent proton transport by the voltage sensor of the *Shaker* K^+ channel. *Neuron*. 19:1319–1327.

Stefani, E., L. Toro, E. Perozo, and F. Bezanilla. 1994. Gating of *Shaker* K^+ channels: I. Ionic and gating currents. *Biophys. J.* 66:996–1010.

Stefani, E., and F. Bezanilla. 1996. Early events in voltage gating. *Biophys. J.* 70:A143 (Abstr).

Tang, C. Y., F. Bezanilla, and D. M. Papazian. 2000. Extracellular Mg^{+2} modulates slow gating transitions and the opening of *Drosophila* ether-à-go-go potassium channels. *J. Gen. Physiol.* 115:319–338.

Tiwari-Woodruff, S. K., M. A. Lin, C. T. Schulteis, and D. M. Papazian. 2000. Voltage-dependent structural interactions in the *Shaker* K^+ channel. *J. Gen. Physiol.* 115:123–138.

Yang, N., A. L. George, Jr., and R. Horn. 1996. Molecular basis of charge movement in voltage-gated sodium channels. *Neuron.* 16:113–122.

Yang, Y., Y. Yan, and F. J. Sigworth. 1997. How does the W434F mutation block current in *Shaker* potassium channels? *J. Gen. Physiol.* 109:779–789.

Zagotta, W. N., T. Hoshi, and R. W. Aldrich. 1994. *Shaker* potassium channel gating. III: Evaluation of kinetic models for activation. *J. Gen. Physiol.* 103:321–362.